

RESEARCH ARTICLE

A systems biology analysis of metastatic melanoma using in-depth three-dimensional protein profiling

Mee-Jung Han^{1,2*}, Huan Wang¹, Lynn A. Beer¹, Hsin-Yao Tang¹, Meenhard Herlyn¹ and David W. Speicher¹

¹ The Wistar Institute, Philadelphia, PA, USA

² Department of Chemical and Biomolecular Engineering, Dongyang University, Punggi-eup, Yeongju, Gyeongbuk, Republic of Korea

Melanoma is an excellent model to study molecular mechanisms of tumor progression because melanoma usually develops through a series of architecturally and phenotypically distinct stages that are progressively more aggressive, culminating in highly metastatic cells. In this study, we used an in-depth, 3-D protein level, comparative proteome analysis of two genetically, very closely related melanoma cell lines with low- and high-metastatic potentials to identify proteins and key pathways involved in tumor progression. This proteome comparison utilized fluorescent tagging of cell lysates followed by microscale solution IEF prefractionation and subsequent analysis of each fraction on narrow-range 2-D gels. LC-MS/MS analysis of gel spots exhibiting significant abundance changes identified 110 unique proteins. The majority of observed abundance changes closely correlate with biological processes central to cancer progression, such as cell death and growth and tumorigenesis. In addition, the vast majority of protein changes mapped to six cellular networks, which included known oncogenes (JNK, *c-myc*, and *N-myc*) and tumor suppressor genes (p53 and transforming growth factor- β) as critical components. These six networks showed substantial connectivity, and most of the major biological functions associated with these pathways are involved in tumor progression. These results provide novel insights into cellular pathways implicated in melanoma metastasis.

Received: July 29, 2009
Revised: June 24, 2010
Accepted: September 10, 2010

**Keywords:**

2-D DIGE / Metastatic melanoma / Microscale solution IEF / Protein networks / Systems biology

1 Introduction

Melanoma is a cancer of the neural crest-derived cells that provide pigmentation to skin and other tissues. Cutaneous melanoma is one of the most aggressive human tumors with rapid metastatic spread, and this cancer has one of the highest

rates of increased incidence over the past several decades. Early-stage melanoma is curable, but the prognosis of individuals with metastatic melanoma is poor, with a 5-year survival rate of approximately 12% [1]. Consequently, the identification of important molecular events involved in the progression of metastatic melanomas is of great clinical significance. However, despite advances made in skin cancer detection and diagnosis, there are no standard biological assays in clinical use that can predict reliably the presence of micrometastases.

The recent advent of comparative large-scale gene expression techniques, such as differential hybridization [2], RNA fingerprinting [3], serial analysis of gene expression

Correspondence: Dr. David W. Speicher, The Wistar Institute, 3601 Spruce Street, Philadelphia, PA 19104, USA

E-mail: speicher@wistar.org

Fax: +1-215-898-0664

Abbreviations: IL-1 β , interleukin-1 β ; JNK, c-Jun N-terminal kinase; MAGE, melanoma antigen gene; MCM, microchromosome maintenance; MicroSol-IEF, microscale solution IEF; TGF- β , transforming growth factor- β ; uPA, urokinase plasminogen activator

*Additional corresponding author: Dr. Mee-Jung Han

E-mail: mjhan75@du.ac.kr

(SAGE) [4], and cDNA microarray technology [5–7] has provided some insights into molecular mechanisms associated with the development and progression of malignant diseases, including melanoma. Consequently, several genes, such as secreted acidic cysteine-rich glycoprotein (SPARC), macrophage migration inhibitory factor (MIF), cathepsin Z (CTSZ) [3], lysophosphatidic acid receptor Edg-2 (EDG2) [6], and ras homolog gene family, member C (RhoC) [7], have been identified as potential markers of metastatic melanomas. However, the phenotype of a given cell is a direct result of functionally active protein levels, and protein abundance does not always correlate with mRNA levels [4]. Furthermore, functional protein activity is often greatly affected by PTMs, such as phosphorylation, proteolytic processing, and other structural modifications, which can be assessed only at the protein level.

Unfortunately, several technical challenges have limited the capacity of quantitative proteome comparisons to provide novel insights into cancer metastasis. The most serious challenge when using proteomics to study tumor progression is that many of the protein-level differences observed between different cancer cell lines are not directly involved in tumor development and instead simply result from aneuploidy and compromised DNA repair pathways. Another major challenge is maximizing the number of proteins that are quantitatively compared. The most common comparative protein profiling method is 2-DE, which has been used for more than 30 years [8] and remains a core protein profiling technology, despite substantial limitations. However, conventional 2-DE and alternative quantitative protein profiling approaches, such as LC/LC-MS/MS methods, typically evaluate only a tiny part of the proteome of cancer cells or tumor tissue. The 2-DE method detects some alternative splice changes and PTM changes, but it can detect only the most abundant cellular proteins, which are typically biologically less interesting than lower abundance regulatory proteins. While alternative protein profiling methods, such as LC/LC-MS/MS, may detect some lower abundance proteins, most non-2-DE methods are very poor at detecting changes in PTMs or splice form changes.

Several prior studies used conventional 2-DE to compare metastatic human melanoma cells with non-metastatic cells [9–11]. For example, Bernard *et al.* [11] compared the proteomes of normal melanocytes with melanoma cell lines and identified eight proteins as differentially expressed in the transformed cells. In particular, hepatoma-derived growth factor (HDGF) and nucleophosmin B23 strongly correlated with melanoma. More recently, combined analysis of proteomic and transcriptomic profiling of murine melanoma progression was used to identify critical proteins and pathways underlying melanoma metastasis [4]. That study showed reductions in several proteins responsible for reactive oxygen species degradation, such as glutathione-S-transferase, superoxide dismutase, aldehyde dehydrogenase, thioredoxin, peroxiredoxin 2, and peroxiredoxin 6 in murine melanoma cell lines compared to the non-tumoral cell, melan-a. Inhi-

bition of the p53 pathway and activation of the Ras and c-myc pathways also were observed.

In the current study, an in-depth comparative proteome analysis of two genetically, very closely related melanoma cell lines was performed using three-dimensional (3-D) DIGE, which we recently showed could substantially enhance proteome coverage when analyzing melanoma cell or lung tissue extracts [12]. We performed a systematic comparison of the primary human melanoma cell line (WM793) with a highly metastatic variant of the WM793 cell line that was selected in athymic mice [13]. Unlike comparisons of unrelated cell lines, comparisons of these two closely matched cell lines minimizes incidental protein changes caused by aneuploidy-related variations and defective DNA repair, thereby focusing on molecular events associated with the metastatic phenotype. Specifically, the vast majority of the observed protein-level changes mapped to cellular pathways and networks known to be involved in cancer progression. In each of these networks, the in-depth proteome analysis resulted in identification of altered protein levels for a substantial number of the proteins associated with the network. This yielded a bimodal distribution where six networks yielded highly significant scores and all other networks were not significantly associated with metastasis. These data suggest that the six networks identified here may define the minimum key cellular events associated with development of the biologically complex metastatic melanoma phenotype.

2 Materials and methods

2.1 Cell culture and sample preparation

A primary human melanoma cell line (WM793) and a highly metastatic variant of the parental cell line (1205LU) selected from WM793 in athymic mice were cultured as described previously [13]. Prior to cell extraction, ~80% confluent cells in 150-mm tissue culture plates were washed three times with PBS (pH 7.4) containing protease/phosphatase inhibitors (0.15 mM PMSF, 2 mM Na₃VO₄, 50 mM NaF, 1 µg/mL leupeptin, 1 µg/mL pepstatin) at 0–4°C. Cells were scraped off plates on ice in PBS, collected by centrifugation, and were lysed by addition of lysis buffer (pH 8.5) containing 8 M urea, 2 M thiourea, 4% w/v CHAPS, and 30 mM Tris followed by sonication. The supernatant was separated by centrifugation at 40 000 × *g* for 30 min at 10°C, protein concentration was determined using a Coomassie Plus protein assay (Pierce Biotechnology, Rockford, IL, USA), and aliquots were stored at –80°C.

2.2 Protein labeling

Proteins were labeled with *N*-hydroxy succinimidyl ester-derivatives of the cyanine dyes Cy3 and Cy5 (GE Healthcare,

Chalfont St Giles, Bucks, UK) following the protocol recommended by the manufacturer for 2-D DIGE. Typically, 400 pmol of Cy3 or Cy5 reagent were added *per* 50 µg of total protein. Labeling reactions were performed on ice in the dark for 30 min, and then quenched with a 50-fold molar excess of 10 mM lysine for 10 min on ice in the dark. The labeled samples were stored at -80°C until needed.

2.3 Microscale solution IEF (MicroSol-IEF) prefractionation

Typically, a Cy3- and a Cy5-labeled sample were mixed and prefractionated using MicroSol-IEF, essentially as previously described [12], using partition membrane disks (ZOOM disks) with pH values of 3.0, 4.6, 5.4, 6.2, 7.0, 9.1, and 12 in a ZOOM IEF Fractionator (Invitrogen, Carlsbad, CA, USA). A total of 1.5 mg of mixed Cy-labeled proteins was separated using maximum limits of 1 mA and 1 W until a maximum voltage of 1200 V was reached. The separation was then continued until a stable low current (~ 0.4 mA) was reached.

2.4 2-D gels

For narrow pH range 2-DE [14, 15], the Cy-labeled aliquots from each MicroSol-IEF fraction were diluted to the required volume using sample buffer containing 8 M urea, 2 M thiourea, 4% w/v CHAPS, 1% w/v DTT, and 1% v/v IPG buffer that matched the pH range of the IPG strips being used. Fractions then were applied to the desired narrow pH range Immobiline DryStrips (GE Healthcare), using either cup-loading or in-gel rehydration following the manufacturer's protocol in an IPGphor (GE Healthcare) using five phases of stepped voltages from 200 to 8000 V, with total focusing of 60 kVh. To improve throughput,

18-cm narrow pH range IPG strips were trimmed to fit Criterion gel cassettes (Bio-Rad, Hercules, CA, USA) by removing the pH range of the IPG strip outside the pH range of the MicroSol-IEF fraction, as shown in Table 1 and as previously described [12]. The trimmed IPG strips were run on 10% Tris-Tricine gels at 165 mA constant current with cooling. In addition, conventional 2-D DIGE was performed in parallel using replicate aliquots of the labeled, mixed, unfractionated samples, which were run directly on broad-range IPG strips (pH 3–11 NL; 11-cm) followed by 10% Criterion Tris-Tricine 2-D gels.

2.5 Image acquisition and analysis

After electrophoresis, Criterion gel cassettes were split and gels were transferred between low-fluorescence glass plates and scanned using a ProXPRESS Proteomic Imaging System (PerkinElmer, Boston, MA, USA) with the following filters: 540/590 nm for Cy3 and 625/680 nm for Cy5. After imaging the Cy-dye signals, the gels were fixed overnight in 40% v/v ethanol and 10% v/v acetic acid, followed by staining with Silver Quest (Invitrogen) to facilitate excising spots of interest. The Cy3/Cy5 gel images were overlaid and merged using ImageMaster 2D Platinum software (version 5.0; GE Healthcare). At least duplicate gels of each fraction were analyzed. Features resulting from non-protein sources were filtered out, protein spots were normalized, and pairwise image comparisons were performed. All protein spots exhibiting at least twofold differences between the cell lines were evaluated for statistical significance comparing duplicate gels for each condition using the Student's *t*-test. All spots with *p* values of < 0.05 were manually inspected to ensure good spot assignment and volume integration. Significantly altered spots were matched with the corresponding spots on the silver-stained images for identification using LC-MS/MS.

Table 1. Summary of results from 2-D and 3-D comparisons of melanoma cell lines

MicroSol Fractions [IPG strip: original pH, length/final length]	Total spots	Significant differences	Identified proteins
Unfractionated sample [pH 3–11, 11 cm/11.0 cm]	1003	15	14
Fractionated sample ^{a)}			
Fraction 1 (3.0–4.6) [pH 3.0–5.6, 18 cm/11.2 cm]	100	8	8
Fraction 2 (4.6–5.4) ^{b)} [pH 4.5–5.5, 18 cm/13.0 cm]	946	38	27
Fraction 3 (5.4–6.2) [pH 5.3–6.5, 18 cm/12.0 cm]	1004	47	47
Fraction 4 (6.2–7.0) [pH 6.2–7.5, 18 cm/11.1 cm]	1245	31	28
Fraction 5 (7.0–9.1) [pH 6–11, 18 cm/7.6 cm]	975	27	26
Fraction 6 (9.1–12) [1-D gel]	50	6	6
Total fractionated sample	4320	157	142 (104) ^{c)}

- a) Fractionated samples F1 to F5 were separated on the very narrow pH range 18-cm IPG strips indicated, which were subsequently trimmed to appropriate pH ranges and run on Criterion gels (13 × 9 cm). Fraction 6 was separated on a 10% NuPAGE Bis-Tris gel and thus the number of detected "spots" is actually the number of bands on the 1-D gel analyzed by using Quantity One software (Bio-Rad).
- b) In fraction 2, the length of the pH 4.6–5.4 region is actually 14.4 cm. After IEF, the middle of this region (~ 13 cm) was cut and separated on a second-dimension Criterion gel. The two remaining edge parts of the IPG strip were run on another 2-D gel to confirm that the loss of proteins in these trimmed regions was very minor.
- c) The number of non-redundant proteins identified from total fractionated samples is given in parenthesis and does not include six identifications unique to the unfractionated sample.

2.6 LC-MS/MS analysis

Gel spots of interest were excised, destained by incubating in 30 mM potassium ferricyanide and 65 mM sodium thiosulfate for 10 min, washed in Milli-Q water until colorless and transparent, vacuum dried, and proteolysed with 0.02 µg/µL of modified trypsin (Promega, Madison, WI, USA) as previously described [16]. Tryptic peptides (typically 8 µL aliquots) were analyzed by LC-MS/MS on a LTQ linear ion trap mass spectrometer (Thermo Scientific, San Jose, CA, USA) interfaced with a NanoLC pump (Eksigent Technologies, Livermore, CA, USA) and cooled autosampler, and resulting data were analyzed using TurboSEQUENT Browser version 27, revision 12 (Thermo Scientific), as follows. The acquired MS/MS spectra were converted to peak lists (DTA files) using minimum ions = 30 and minimum TIC = 3000. The DTA files were searched against a composite International Protein Index human and mouse database (version 3.03) that included the sequence of the trypsin and a concatenated copy of the reversed database (total forward entries = 91 357). Prior to searching the database with SEQUEST, it was indexed using: monoisotopic mass range of 500–3500, length of 6–100 residues, full tryptic cleavage with one allowed internal missed cleavage, static modification of Cys by carboxamidomethylation (+57 Da), and dynamic modification of Met to methionine sulfoxide (+16 Da). The DTA files were searched with a 2.5-Da precursor mass tolerance and 1-Da fragment ion mass tolerance. Other search parameters were identical to those used for database indexing.

SEQUEST Browser was used as previously described [16] for further data analysis and filtering, which utilized HUPO-defined criteria for high-confidence peptide identifications, *i.e.* $X_{\text{CORR}} \geq 1.9$ ($z = 1$), 2.2 ($z = 2$), 3.75 ($z = 3$), and $\Delta C_n \geq 0.1$; and $R_{\text{SP}} \leq 4$ [17]. Keratins were excluded from all datasets as likely contaminants. Different forms (charge states and Met oxidation) of an identified peptide were counted as a single peptide hit, and peptides that were subsets of a larger peptide were counted as a single peptide. However, if two peptides partially overlapped, they were counted separately. Protein identifications in very low-abundance spots that were based on a single, unique, high-confidence peptide assignment were retained only if expert inspection of the MS/MS spectra supported the identification and either the protein was identified in a proximal spot with additional peptides, or if there was good agreement between observed and theoretical pI and MW. When more than one protein was identified in a 2-D gel spot, the human protein with the highest score in Proteomics Browser (*i.e.* sum of the S_f scores for each peptide identified) and with at least sixfold higher TIC between the top and second rank protein was selected as the most likely protein responsible for the observed signal intensity change. If the scores were very similar and/or there was a less than sixfold difference of TIC between the two top-ranked proteins, the protein identification was regarded as ambiguous and was not considered

further in this study. Similarly, in a few cases where a human protein was not identified, the identification was regarded as ambiguous and was not considered further in this study.

2.7 Semi-quantitative Western blots

Protein levels of selected proteins of interest were verified using semi-quantitative Western blots. Briefly, aliquots of WM793 and 1205LU cell lysates were thawed, and multiple protein concentrations of each cell line (20, 10, and 5 µg, respectively) were separated on 12% Bis-Tris NuPAGE gels (Invitrogen). Proteins were transferred to Immobilon-P PVDF membranes (Millipore, Billerica, MA, USA), membranes were stained with MemCode reversible protein stain (Pierce Biotechnology) and imaged to verify uniform protein loads and efficient electrotransfer, and membranes were destained with Milli-Q water and blocked with non-fat dry milk or BSA prior to incubation with the following primary antibodies: anti-Cathepsin D mAb (Sigma-Aldrich, St. Louis, MO, USA), anti-Lamin B mAb (Invitrogen), anti-Cathepsin B pAb (Calbiochem, San Diego, CA, USA), anti-Galectin pAb (Invitrogen), anti(total)-JNK (Cell Signaling), anti-phosphorylated-JNK (Cell Signaling), anti-interleukin-1β (R&D systems), anti-c-Myc (Cell Signaling), anti-MCM2 (Cell Signaling), and anti-MAGED2 (Abnova). HRP-labeled secondary antibodies and SuperSignal West Pico Chemiluminescent Substrate (Pierce Biotechnology) were used. X-ray film images were background subtracted and protein bands were quantitated using The Discovery Series Quantity One 1-D Analysis software (Bio-Rad).

2.8 Network analysis

Protein accession numbers identified by LC-MS/MS analysis and their corresponding fold changes were imported into the Ingenuity Pathway Analysis software (Ingenuity® Systems, www.ingenuity.com) for network analysis. The identified proteins were mapped to networks available in the Ingenuity database and then ranked by score. The score is the probability that a collection of genes equal to or greater than the number in a network could be achieved by chance alone. A score of 3 indicates that there is a 1/1000 chance that the focus genes are in a network due to random chance.

3 Results

3.1 Proteome profiles of metastatic melanoma cells

Typically, 1 mg of total protein extracts from WM793 and 1205LU melanoma cells were labeled with either Cy5 or Cy3 and then mixed together. A total of 1.5 mg of the mixed Cy-labeled samples was subjected to fractionation by

MicroSol-IEF followed by narrow pH range 2-D gels. Another aliquot of the mixed Cy-labeled sample was analyzed in duplicate without fractionation, *i.e.* the traditional 2-D DIGE method (Fig. 1A). The most abundant melanoma cell proteins, which were detectable using conventional 2-D DIGE, displayed a striking bimodal distribution, with the densest clusters of spots occurring between pH 4.7–6.2 and pH 6.7–9.1. Quantitative analysis of 2-D DIGE images (unfractionated sample) showed approximately 15 protein spots with significant abundance changes between cell lines could be detected at this level of analysis.

To achieve a greater depth of analysis and higher resolution of these proteomes, the mixed Cy-labeled cell extracts also were separated into six fractions using MicroSol-IEF. Fractions 1–5 were well separated, with most observed spots

migrating within the expected pH ranges when analyzed on narrow-range 2-D gels (Fig. 1B–F). Fraction 6, which contained the fewest proteins, could not be well resolved when separated on 18-cm IPG strips between pH 9.1 and 12, as is typically the case for very basic proteins. Due to the low complexity of this fraction, in subsequent experiments it was concentrated fivefold by acetone precipitation and separated on a 10% 1-D gel (Fig. 1G). The narrow pH range 2-D gels showed that the majority of proteins were recovered in fractions 2–5, which include pI's between 4.6 and 9.1. These results are consistent with the protein distributions observed in the 2-D gels of the unfractionated samples. The effective total IEF separation distance of fractions between pH 3 and 9.1 was about 55 cm. Hence, detection of lower abundance proteins was facilitated by both the greatly increased IEF separation distance and the higher protein

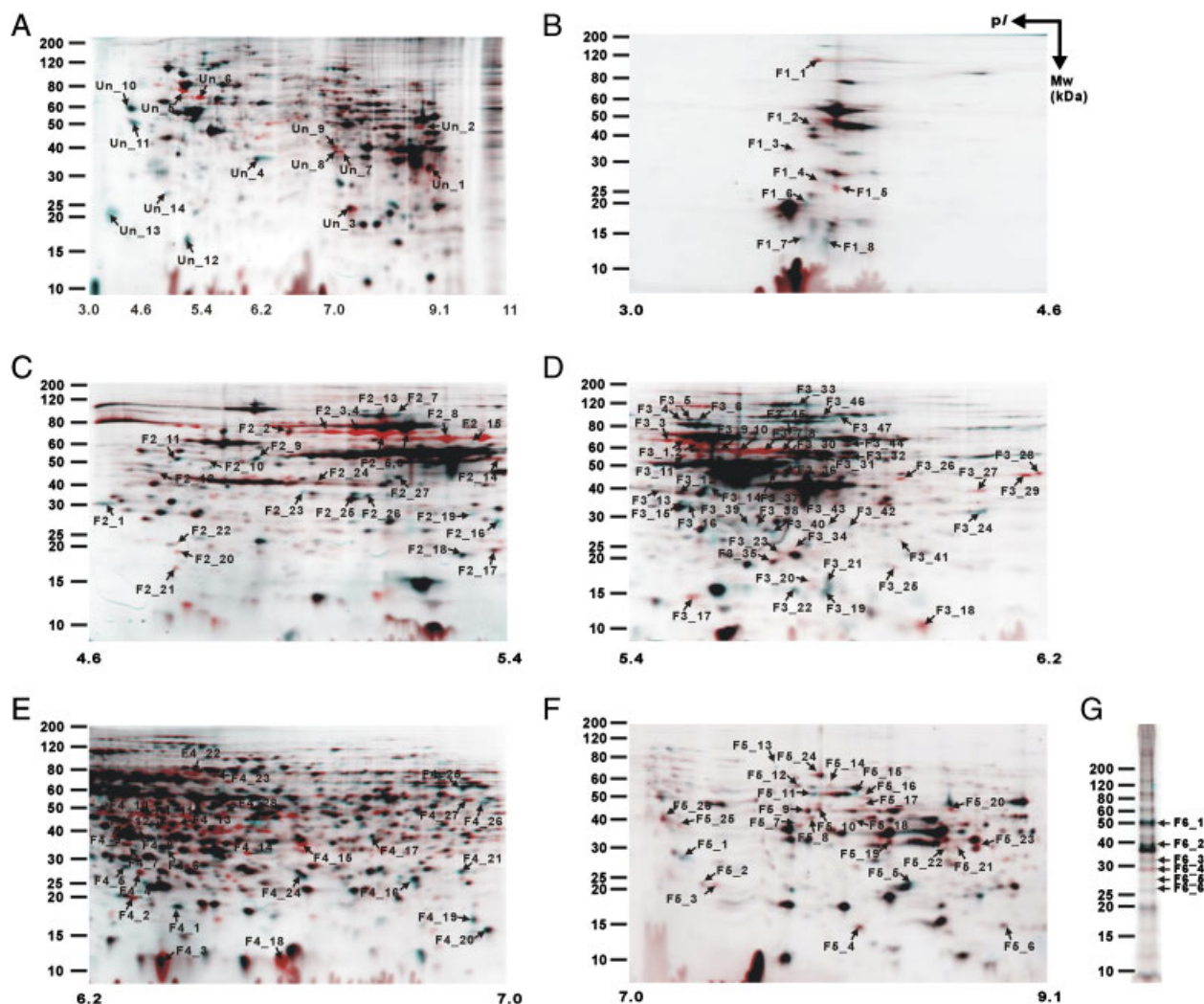


Figure 1. Composite merged images from 3-D DIGE comparison of melanoma cells with low- and high-metastatic potential. Gel images were merged by overlaying Cy3-labeled 1205LU (blue) and Cy5-labeled WM793 melanoma cell (red) images. (A) A broad pH range 2-D gel of unfractionated samples, (B–F) narrow pH range 2-D gels of MicroSol-IEF fractions 1–5, and (G) a 1-D gel of MicroSol-IEF fraction 6. The positions of spots showing significant abundance changes that were excised for protein identification using LC-MS/MS are indicated.

loads that could be applied to narrow-range gels after pre-fractionation as previously demonstrated [14, 15, 18].

To identify proteins implicated in melanoma metastatic potential, data from two independent MicroSol fractionations and duplicate gels of each fraction from these two separations were analyzed. Protein spots that changed by at least twofold and also showed statistically significant differences having p values of <0.05 between primary and metastatic melanoma cells were further analyzed. First, spot matches, boundaries, and quantitations were verified by manual inspection. Properly integrated, significantly changed spots subsequently were excised, digested with trypsin, and analyzed by nLC-MS/MS. On the basis of these criteria, a total of 172 protein spots, including the 15 spots from the unfractionated gel and 157 spots from the fractionated narrow-range 2-D gels, were analyzed (Table 1). A total of 110 unique proteins were unambiguously identified, as well as multiple isoforms of some proteins, which in most cases were presumably due to changes in PTMs. Of the 110 non-redundant identified proteins, 42 were present at increased levels in highly metastatic melanoma cells, while 68 showed decreased levels (Supporting Information Table 1). A more detailed summary of the proteome analysis, including peptide sequence information and theoretical and observed molecular mass and pI values of identified proteins, are presented in Supporting Information Table 2. Identifications of 34 spots from the 3-D DIGE analysis were to proteins with known multiple splice forms. For 15 of these protein spots, unique splice forms could be unambiguously assigned due to identification of splice form-specific peptide sequences. Each unique sequence is highlighted with a yellow background in Supporting Information Table 2. Consistent with our previous study, these results show that, in some cases, the 3-D DIGE method can effectively separate and distinguish between multiple closely related splice forms [12]. While many of the observed changes in spot intensities are likely due to changes in abundance of the identified protein, some of the detected changes are most likely due to changes in levels of PTMs that result in detectable shifts of either the pI or apparent size of the protein, such as phosphorylation or glycosylation (see Supporting Information Table 2).

3.2 Verification of selected protein changes using semi-quantitative Western blots

Semi-quantitative Western blots were performed for several proteins that exhibited moderate abundance changes in the 3-D proteome analysis to independently evaluate the reliability of the 3-D DIGE proteomics results. Initially, commercially available antibodies with appropriate reported specificity for six proteins with moderate observed abundance changes were selected. Westerns were performed using serial dilutions of WM793 and 1205LU cell extracts from different batches of cells than those used for the 3-D DIGE experiments. Two antibodies showed high, non-

specific background despite repeated attempts to optimize the assay. Westerns for the four remaining antibodies were optimized and signals within the linear range of the assays from identical protein loads for the two cell lines were used for estimating the fold change in the metastatic cells. Representative results are shown in Fig. 2A. As indicated, Western results were generally consistent with results from the 3-D DIGE analysis. That is, the direction of the observed changes (higher or lower in metastatic melanoma) using both methods was consistent, although the magnitude of the change was substantially different for galectin.

3.3 Protein network analysis

We systematically evaluated the 110 non-redundant proteins exhibiting abundance changes associated with metastatic potential by performing protein network analyses using Ingenuity Pathway Analysis, a gene-based tool that extracts biologically relevant information from genomic and proteomic studies by correlating individual proteins (genes) with biological processes, cellular pathways, and regulatory networks based on known interactions extracted by the software vendor from the scientific literature [19, 20]. The 110 genes corresponding to the unique proteins identified in this study, and their corresponding observed fold changes,

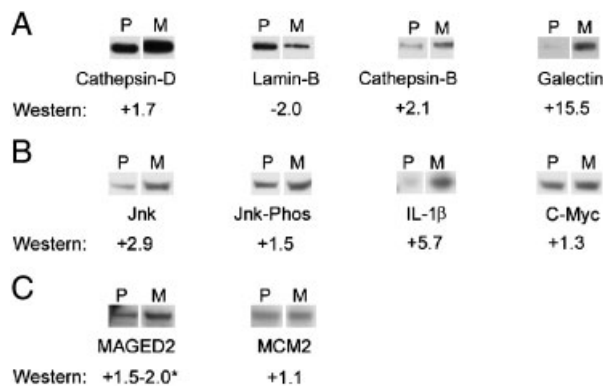


Figure 2. Representative Western blots of proteins in primary and metastatic melanoma cell lines. Equal amounts of total protein from the primary melanoma cell line WM793 (P) and metastatic cell line 1205LU (M) were compared as described in Section 2. The fold change in protein level in the metastatic cell line compared to the primary cell line is shown for the illustrated Western blots. (A) Verification of protein changes observed using the 3-D DIGE method. The corresponding fold changes from the 3-D DIGE analyses were cathepsin-D ± 2.1 and $+3.0$; lamin B 2.0 ; cathepsin-B ± 2.2 and $+5.3$; and galectin-1 ± 2.1 and $+2.4$ (see Supporting Information Table 1). (B) Comparisons of central proteins in top scoring networks. Changes in JNK and c-Myc were not detected in the 3-D DIGE analysis. The corresponding fold change from the 3-D DIGE analysis for IL-1 β was -2.0 (see Supporting Information Table 1). (C) Analysis of undetected proteins that were previously associated with metastatic melanoma.

Table 2. The top six networks generated by the Ingenuity Pathway Analysis for metastatic melanoma

Network ID	Molecules in network ^{a)}	Score	No. of focus genes	Top 3 functions
1	<u>Actin</u> , ANXA2 , Caspase, Ck2, CTSB , EEF1A1 , G6PD , HNRPA2B1 , HNRPC , HNRPK , <u>Hsp70</u> , HSPA5 , HSPB1 , HYOU1 , IL1 , IL1B , Jnk, LMNB1 , Mmp, NPM1 , NQO1 , <u>PP1/PP2A</u> , PPP1CA , PPP1CB , PPP2R1A , PRDX1 , PRDX4 , PSME2 , S100A4 , SERPINB2 , SERPINH1 , SOD2 , STIP1 , TALDO1 , TPT1	56	27	Cell death Cancer Endocrine system disorders
2	ACTA1 , ACTB , ACTN4 , CD9, CREBBP, CTSD , DHFR, ERBB2, EWSR1, FADS2, GAPDH, GTF2I, HSPH1 , INS1 , LDHB , LIMK1, MRPL12 , MYC, MYL9 , PABPC1, PBX1, PDIA4 , PHB , PPP2R5A , PRDX2 , PSAP , PSAT1 , PTMS , RPS12 , SHMT2 , SOD2 , STRAP , TFAP2A , UQCRC2 , VIM	32	18	Cancer Gene expression Cell cycle
3	ACTB , ALDOA , C19ORF10 , COL1A1, DDIT3, EGFR, EIF4A1 , EIF4G2, EIF5A , FABP7 , FKBP9 , HSPD1 , IFNG, LEPRE1 , LGALS1 , MAX, MIF, MUC1, MYCN, NUP98, PABPC1, PBX1, PHGDH , PLD1, PLD2, PLK1, PSMA7 , PSMC3 , RPL5, SSBP1 , TPI1 , TXN, Ubiquitin, USP5 , VIM	30	17	Cellular growth and proliferation Cancer Cell death
4	2-methoxyestradiol, ACAT1 , AK3 , APP, BACE1, BCL2L1, CALM , CASP7, CCNE1, cholesterol, CYB5B , CYP17A1, EEF1D , GNAO1 , HADH , HSPA5 , IDI1, IL1RN, ITPR1, KPNA6 , LEP, linoleic acid, MSR1, NFATC2, PRPS1 , RPLP2 , SERPINF1, SOD2 , SPFH2 , TG, TGFB1, TNFSF11, UGP2 , VDAC3 , XBP1	25	15	Cell death Immunological disease Free radical scavenging
5	ACTB , ACTL6B , AKR1B1 , ARID1A, ARPC5 , Ca ²⁺ , CALU , CCT4, CCT7 , CCT8, CCT6A, COTL1 , CS , CYB5A , D-glucose, F Actin, FTL , glutamine, GNAI3 , GSN , HNRPC , HPCAL1, HTR2C, ITPR3, KNG1, MDH2 , NR3C1, PPARGC1A, S100A11 , SCIN, SMARCA4, SMARCD1, SMARCD3, TKT , VDAC1	25	15	Cellular assembly and organization Post-translational modification Cellular compromise
6	Adenosine-tetraphosphatase, Akt, ANP32A , ATP5A1 , ATP5H , ATP6V1A , ATXN1, AURKA, CALR , CD28, CD247, CD40LG, GAB2, GAPDH, GRSF1 , H ⁺ -transporting two-sector ATPase, H2-ALPHA, Histone h3, HSPD1 , hydrogen peroxide, KLF4, LOC112714, MKNK1, NASP , P38 MAPK, PRDX6 , TARDBP , TST, TUBA1 , TUBA6 , TUBA8, TUBB, TUBB1, TUBB4, UBQLN4	21	13	Cancer Reproductive system disease Dermatological diseases and conditions

a) Proteins exhibiting significant changes in abundance and their corresponding fold change in metastatic melanoma were used as input for the Ingenuity program and are shown in bold. In several cases (gene or protein name underlined), a close homologue was identified and the homologous protein was color coded in the corresponding networks but was not defined as a focus gene. For each network the score indicates the likelihood the focus genes would have been found by random chance (see Section 2). The number of focus genes in the network and the three most significant biological functions are shown.

were mapped to cellular networks using this software/database tool. The resulting networks and pathways were produced automatically by the software and were not manually modified. Six networks were very highly significant, with scores greater than 20. Interestingly, there was a sharp delineation in the network scores, as all other networks had scores of less than 3, *i.e.* below the significance threshold. The score, number of focus genes, and top three biological functions for each of the six significant networks are shown in Table 2. These six networks contained a total of 192 genes, and 97 of these genes showed significant abundance changes of the corresponding protein in this study. These differentially expressed proteins/genes are considered “focus genes.” All six networks are implicated in biological functions expected to be critically

involved in tumor progression, and at least five of the networks include cancer (Networks 1, 2, 3, and 6) and/or cell death (Networks 1, 3, and 4) among the top three associated functions. Interestingly, Network 6 is closely associated with dermatological diseases and conditions.

Diagrammatic representations of the top network, with a significance score of 56 and 27 focus genes out of a total of 35 genes and the second network with a score of 32 and 18 focus genes out of a total of 35 genes, are shown in Figs. 3 and 4, respectively. The four other significant networks are shown in Supporting Information Figs. 1–4. The shaded genes are those identified in this study and symbols outlined in orange are the proteins previously implicated in cancer. This clearly shows that the 3-D DIGE analysis used here has extended the association of those pathways with melanoma metastasis to a

substantial number of additional genes/proteins. In Network 1, the differential expression of interleukin-1 β (IL-1 β) in melanoma cells may interact with c-Jun N-terminal kinase (JNK) and influence its downstream targets, such as SERPINB2, SERPINH1, CTSB, HSPB1, and HSP70 (Fig. 3). The differential accumulation of proteins involved in oncogene/tumor suppressor pathways was observed primarily in Networks 2, 3, and 4. This analysis of these gene/protein networks suggests the myc family (*c-myc* and *N-myc*) and other oncogenes may be relevant not only for the regulation of intrinsic cell functions, but also may play critical roles during development of metastatic melanoma. Furthermore, this analysis has identified additional proteins implicated in

cell death or tumorigenesis that are likely to be important players in metastatic melanoma development.

3.4 Evaluation of selected critical protein changes using semi-quantitative Western blots

Several central proteins in the two top scoring networks (JNK and c-Myc) were not detected by the proteomics analysis, and IL-1 β , another central protein in the top network was observed to be reduced in metastatic cells using the 3-D DIGE method when an increased level of intracellular form of this protein would be expected. Hence,

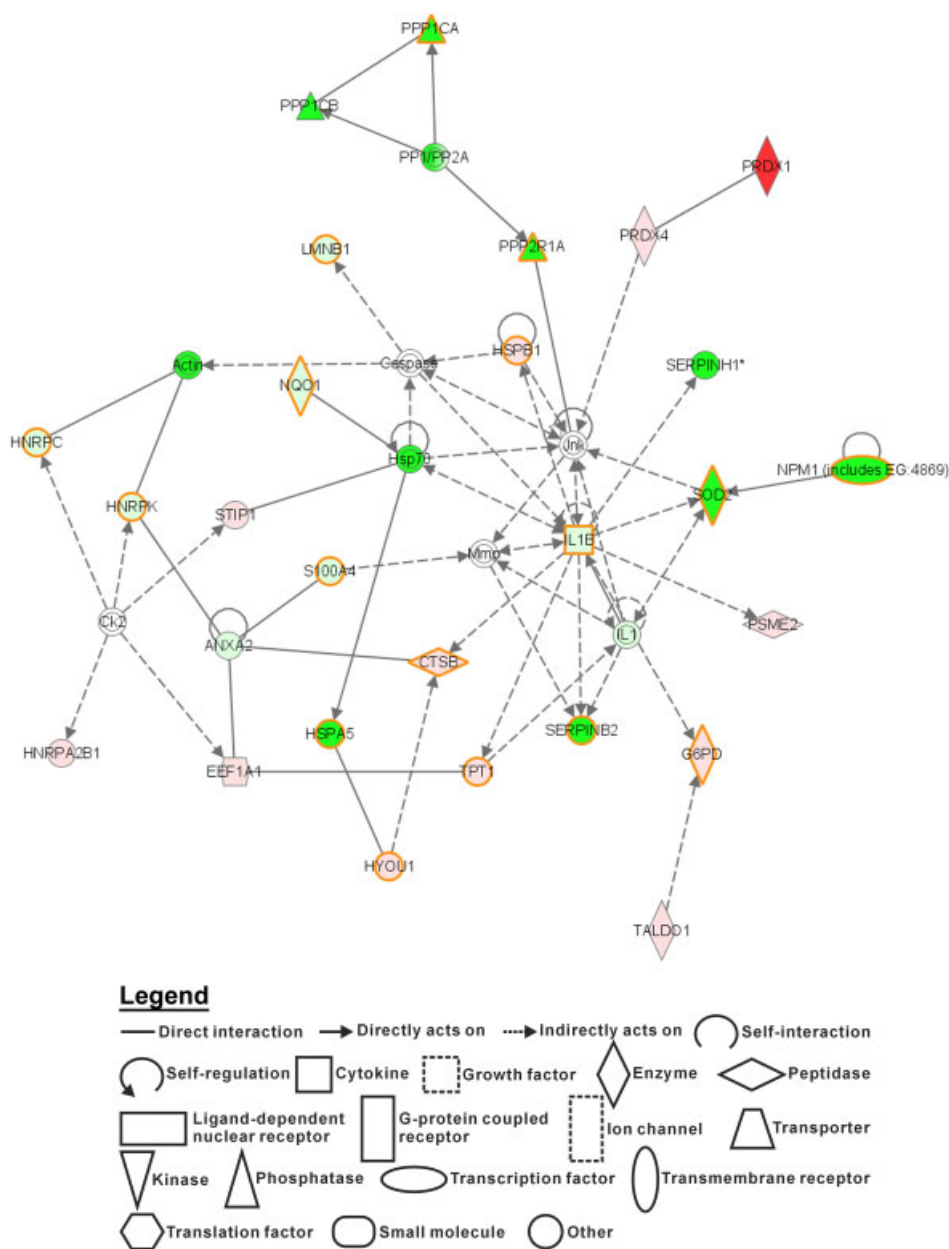


Figure 3. The top-scoring network created by Ingenuity Pathway Analysis. This network exhibited metastatic potential associated abundance changes for at least 27 of the 35 proteins in this network. Shaded genes are those identified in this study with color intensities representative of abundance changes in highly metastatic melanoma cells as follows: red ≥ 100 -fold increase; shades of pink 2- to 100-fold increase; dark green ≥ 100 -fold decrease; shades of green 2- to 100-fold decrease. The meaning of node shapes is defined in the legend. Some networks include metabolites as indicated by the symbols legend. The orange outlines on pathway shapes highlight proteins (genes) previously implicated in cancer. The software and/or the proteomics data did not consistently distinguish between protein family members and therefore in a few cases proteins were highlighted if a closely homologous protein was identified in the 3-D analysis.

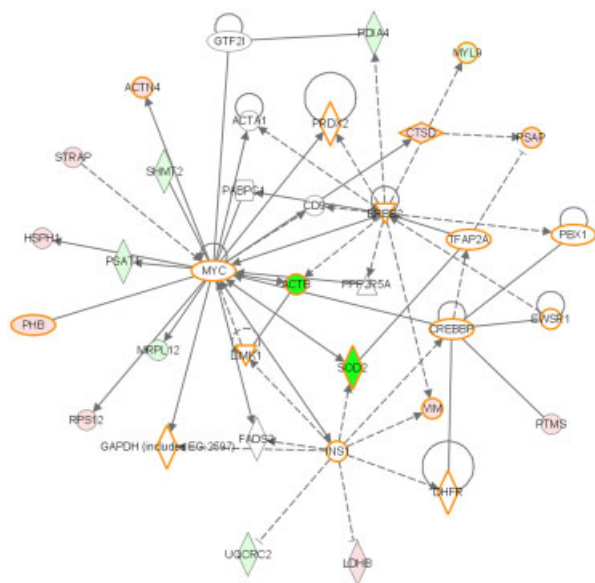


Figure 4. The second highest scoring networks created by Ingenuity Pathway Analysis. This network exhibited metastatic potential associated abundance changes for 18 of the 35 proteins in this network. Additional details are described in the legend of Fig. 3.

Western blots were performed for JNK, Phospho-JNK, IL-1 β , and C-Myc. As shown in Fig. 2B, JNK and IL-1 β were increased substantially in the metastatic cells, while the amount of c-Myc and the phosphorylation level of JNK were increased only marginally in the metastatic cells.

Interestingly, neither the proteome analysis nor the subsequent network analyses identified several antigens previously associated with metastatic melanoma such as the microchromosome maintenance (MCM) family and the melanoma antigen gene (MAGE) family [21]. When representative members of these protein families were evaluated using semi-quantitative Western blots (Fig. 2C), MAGE-D2 exhibited a nearly twofold elevation in the metastatic cells. In contrast, the MCM 2 isoform, which is the most extensively evaluated member of the MCM family, did not show significant changes between the primary and metastatic melanoma cells. This latter result is consistent with a recent immunohistochemistry analysis of tissue sections that showed significant increases of MCM 2 in melanoma cells compared with nevi, but no significant difference between primary and metastatic melanomas [22].

4 Discussion

Melanoma progression is a multistep process involving an incompletely characterized sequence of genetic events affecting multiple biological processes, including control of the cell cycle, apoptosis, enzymatic hydrolysis of the extracellular matrix, local immunosuppression and mechanisms of immunological escape, angiogenesis, and cell migration.

In addition, there may be some similarities in biological mechanisms implicated in melanoma progression and those that play a role in development of drug resistance in malignant melanoma. For example, proteins involved in chemoresistance of malignant melanoma cells, such as elongation factor 1- δ , translationally controlled tumor protein, 60 kDa heat shock protein, and nucleophosmin [23, 24] were differentially expressed in metastatic melanoma.

In this study, we used genetically, very closely related cell lines with differing metastatic potential to minimize incidental genetic noise, *i.e.* incidental protein abundance changes unrelated to tumor progression resulting from impaired DNA repair and variations in chromosomal aberrations that affect gene expression. This goal appears to have been achieved because when we integrated observed protein changes into cellular networks using the knowledge-based Ingenuity Pathway Analysis tools, the vast majority of identified proteins (97/110) mapped to a total of six highly significant cellular networks. Importantly, the top functions associated with these six networks closely correlated with known important cancer progression mechanisms. This strongly suggests that a majority of the observed protein abundance changes are likely to contribute directly to the metastatic phenotype. Furthermore, there was a clear delineation between these six high-scoring networks and the next best-scoring network, which had a score less than three (not significant). The fact that most observed protein changes map to only six highly significant cellular networks with no marginally significant networks is another indication that the greater depth of analysis for our 3-D protein profiling method and the genetically similar cell lines have resulted in identification of primarily those proteins directly implicated in melanoma progression. The highly comprehensive analysis of the current study is reflected further in the fact that approximately half of the proteins in the top networks were shown to change with metastatic potential in this study. In addition, these networks defined additional proteins that were not previously implicated in cancer metastasis.

The Ingenuity Pathway Analysis resource provides a useful method of integrating complex datasets discovered using global genomic or proteomic approaches, as illustrated above. Of course, an inherent weakness of this software and associated Knowledge database is its limitation to those proteins with assigned annotations or published relationships and, as a result, some annotations ultimately may prove to be inaccurate or incomplete. In addition, these networks do not directly define how the changes in levels of specific proteins will affect overall function. In this regard, it should be noted that in all identified networks, some proteins were elevated in metastatic cells while others showed reduced levels. Such opposite changes in a network are expected, as some proteins inhibit a pathway and others activate that function. Similarly, in a network, the stimulatory and inhibitory affects of different components are even more complex. Furthermore, as shown in Fig. 2, Western

blots of total protein levels usually correlate with changes observed on 2-D gels, but there are exceptions such as IL-1 β , which showed a substantial increase in the metastatic cells by Western blot (+5.7-fold), but a twofold decrease for a 2-D gel spot identified as IL-1 β (Supporting Information Table 2). The most likely explanation for this discrepancy is that the 2-D gel analysis probably identified a minor form of IL-1 β as suggested by the observed higher than expected molecular weight (Supporting Information Table 2). In addition, the change in the major form of the protein indicated by the Western blot may have been missed by the 3-D DIGE method due to interference from a more abundant protein or other 2-D gel artifact. This illustrates that while 2-D gels are superior to most alternative proteomics methods in identifying some protein modifications, it often is ambiguous as to whether an observed change reflects the overall abundance of that protein or only a minor form of the protein. Furthermore, although the 3-D DIGE method detects far more proteins than conventional 2-D gels, some proteins such as membrane proteins and proteins larger than 100 kDa are likely to be systematically missed because these groups of proteins are not well recovered from 2-D gels. Also, some relatively low-abundance proteins such as the MAGE proteins may be obscured by other more abundant proteins.

Despite the above caveats, examination of the identified networks shows that most of the results from the current study are both consistent with prior knowledge of tumor progression and, at the same time, substantially expand our knowledge. For example, in Network 1 (Fig. 3), IL-1 β , which plays a critical role in melanoma progression [25], is a central node and directly interacts with 12 other proteins in the network. IL-1, a family of two major agonistic proteins, IL-1 α and IL-1 β , is pleiotropic and affects mainly inflammation, immunity, and hemopoiesis. IL-1 is abundant at tumor sites, where it may affect the process of carcinogenesis, tumor growth and invasiveness, and also the patterns of tumor-host interactions. It has been proposed that membrane-associated IL-1 α expressed on malignant cells stimulates anti-tumor immunity, while secretable IL-1 β , derived from the microenvironment or the malignant cells, activates inflammation that promotes invasiveness and also induces tumor-mediated suppression [26]. Consistent with this role, our Western blot analysis showed that the intracellular level of IL-1 β is elevated in the metastatic cells, although it remains to be determined whether this results in increased levels of secreted IL-1 β . The differential expression of IL-1 β in melanoma cells may interact with JNK and influence its downstream targets as shown in Fig. 3. JNK, which is among the major subgroups of mitogen-activated protein kinase (MAPK), is activated primarily by inflammatory cytokines and environmental stress [27]. A role for the JNK pathway in tumorigenesis is supported by the high levels of JNK activity found in several cancer cell lines [28] and we confirmed using Western blots that JNK is indeed elevated in the metastatic cells in this study. A further

example of a role for JNK in tumorigenesis has been reported in the liver, where JNK was shown to promote chemically induced hepatocarcinogenesis [29].

In Network 2, Myc represents a central biological theme of cancer as well as a central node of this network. Its ability to activate or repress, either directly or indirectly, core genes in the other networks demonstrates that Myc can regulate multiple subsets of genes to elicit specific regulatory programs. Myc plays an important role in regulating cell cycle, cell growth, differentiation, apoptosis, transformation, genomic instability, and angiogenesis, presumably through its ability to activate or repress transcription of target genes that mediate these various processes [30]. Amplification of *myc* genes has been found in a variety of tumor types including lung (*c-myc*, *N-myc*, *L-myc*), colon (*c-myc*), breast (*c-myc*), and neuroblastoma (*N-myc*) [31]. In melanoma, high *c-myc* expression has been found to be associated significantly with vertical growth phase, poor prognosis, and metastases [31]. However, our Western blots indicate that the increase in C-Myc is marginal (Fig. 2B). More interestingly, N-Myc (designated MYCN in Network 3, see Supporting Information Fig. 1) amplification is associated with a variety of tumors, most notably neuroblastomas. Many differentially expressed proteins that are directly connected to the oncogene are translation factors and ribosomal proteins. The ribosomal proteins, including 40S ribosomal protein S12 and 60S acidic ribosomal protein P2, were increased in metastatic cells, which is consistent with previous results from gene expression profile analysis [32]. Furthermore, proteins involved in translation, such as the eukaryotic translation initiation factor 5A and eukaryotic translation elongation factor 1- α and 1- δ , were increased in metastatic melanoma, although eukaryotic initiation factor 4A-I was significantly decreased. These genes have been shown to respond to the *N-myc* oncogene, suggesting that MYCN functions as a major regulator of protein synthesis [33]. The possible involvement of the MYCN proteins in the etiology of common human cancers has raised exciting questions and is the subject of intense investigation by multiple laboratories. The network analyses performed here suggest a common mechanism involving regulatory networks may be involved in human cancers. Of possible significance is the fact that both neuroblastoma and melanoma tumors are derived from the same neural crest progenitor cells [34]. The molecular dissection of how MYCN is involved in human melanoma is an exciting and challenging endeavor that should lead to a better understanding of melanoma metastasis and, perhaps, tumorigenesis.

As expected, proteins associated with tumor invasion and metastasis, including proteases and protease inhibitors, were more likely to be elevated than decreased in metastatic melanoma cells. Specifically, we found cathepsin B and D to be increased in metastatic melanoma by both the 3-D DIGE and Western blot analyses. Both proteins were apparently the processed mature forms when compared with observed

and theoretical molecular masses (Supporting Information Table 1: F3_40 for cathepsin B and F3_39 for cathepsin D). Specific cathepsin proteins, including B and D, have been analyzed extensively and implicated in various cancers [35–38]. Consistent with the observed increased levels of these proteases in the metastatic cells, multiple protease inhibitors exhibited decreases, including plasminogen activator inhibitor-2; serpin peptidase inhibitor, clade B (ovalbumin), member 2 (SERPINB2); serine (or cysteine) proteinase inhibitor; serpin peptidase inhibitor, clade H (heat shock protein 47), member 1; and SERPINH1. In particular, the urokinase plasminogen activator (uPA) system, including the serine protease (uPA), 2 serpin inhibitors (PAI-1 and PAI-2), and the membrane-linked receptor (uPAR), plays a key role in cancer invasion and metastasis [39]. In addition to mediating invasion and metastasis as a result of extracellular matrix dissolution, uPA has been shown to enhance cell proliferation and migration and to modulate cell adhesion. Elevated PAI-2 has been shown to prevent invasion and metastasis of various cancer cells including melanoma [40, 41]. Thus, the observed decreased level of this and other proteinase inhibitors should enhance the proteolytic processes that promote tumor invasion and metastasis. The degradation of basement membranes by tumor cells involves secretion and activation of these proteinases and results from an imbalance between their inhibitors and activators, which are controlled by various growth factors or cytokines. Among them, the transforming growth factor- β (TGF- β) family, centered mainly on Network 4, is one of the most intriguing because it has been reported either to decrease or promote cancer progression. Thus, TGF- β 1 triggered a large decrease of uPA and tPA, as well as a decrease of uPA and uPAR mRNAs, and also induced a strong increase of PAI-1 synthesis [42]. TGF- β 1 may inhibit melanoma tumor growth by specifically decreasing plasmin activity of tumor cells and play a protective role during the earliest stages of tumor progression.

On the other hand, proteins associated with apoptosis and tumor suppressors were decreased in metastatic melanoma (Fig. 3). Although tumor development involves many other processes, in almost all instances, deregulated cell proliferation and suppressed cell death provide the underlying platform for tumor progression. In most cancers, this ability to survive results in part from inhibition of the p53 pathway, either by activating mutations in p53 itself, or perturbation of the signaling pathways that allow activation of p53 in response to stress, or defects in the downstream mediators of p53-induced apoptosis [43]. In this study, we observed a decrease in metastatic melanoma of NAD(P)H dehydrogenase 1 (NQO1), which destabilizes p53 and contributes to increased tumorigenesis of melanoma [44].

Further experiments will be required to unravel the most critical protein changes associated with alternative pathway preferences leading to invasion and metastasis in melanoma and to identify any other discrepancies between apparent

changes in 2-D gel spots and the overall abundance of a given protein, analogous to IL-1 β . Due to the limited availability of specific antibodies, as well as the limited quantitative accuracy of Western blots and their limited throughput, the next logical step is to use targeted multiple reaction monitoring MS to quantitatively assess all proteins in the top-scoring networks defined in this study to further explore the relationships between these networks and the metastatic phenotype.

This work was supported by National Institutes of Health Grants CA93372 and CA92725, as well as institutional grants to the Wistar Institute including an NCI Cancer Core Grant (CA10815), and grants from the Pennsylvania Department of Health. We gratefully acknowledge the assistance of the Wistar Institute Proteomics Facility for conducting LC-MS/MS analyses as well as the technical assistance of Peter Hembach and Michaeline Hebron.

The authors have declared no conflict of interest.

5 References

- [1] Jemal, A., Murray, T., Ward, E., Samuels, A. *et al.*, Cancer statistics, 2005. *CA Cancer J. Clin.* 2005, 55, 10–30.
- [2] Weterman, M. A., Stoop, G. M., van Muijen, G. N., Kuznicki, J. *et al.*, Expression of calyculin in human melanoma cell lines correlates with metastatic behavior in nude mice. *Cancer Res.* 1992, 52, 1291–1296.
- [3] Rumpler, G., Becker, B., Hafner, C., McClelland, M. *et al.*, Identification of differentially expressed genes in models of melanoma progression by cDNA array analysis: SPARC, MIF and a novel cathepsin protease characterize aggressive phenotypes. *Exp. Dermatol.* 2003, 12, 761–771.
- [4] de Souza, G. A., Godoy, L. M., Teixeira, V. R., Otake, A. H. *et al.*, Proteomic and SAGE profiling of murine melanoma progression indicates the reduction of proteins responsible for ROS degradation. *Proteomics* 2006, 6, 1460–1470.
- [5] Bittner, M., Meltzer, P., Chen, Y., Jiang, Y. *et al.*, Molecular classification of cutaneous malignant melanoma by gene expression profiling. *Nature* 2000, 406, 536–540.
- [6] Baldi, A., Battista, T., De Luca, A., Santini, D. *et al.*, Identification of genes down-regulated during melanoma progression: a cDNA array study. *Exp. Dermatol.* 2003, 12, 213–218.
- [7] Clark, E. A., Golub, T. R., Lander, E. S., Hynes, R. O., Genomic analysis of metastasis reveals an essential role for RhoC. *Nature* 2000, 406, 532–535.
- [8] O'Farrell, P. H., High resolution two-dimensional electrophoresis of proteins. *J. Biol. Chem.* 1975, 250, 4007–4021.
- [9] Easty, D., Hart, I. R., Patel, K., Seymour, C. *et al.*, Changes in protein expression during melanoma differentiation determined by computer analysis of 2-D gels. *Clin. Exp. Metastasis* 1991, 9, 221–230.

- [10] Eberle, J., Garbe, C., Kroumpouzos, G., Orfanos, C. E., Protein patterns of benign and malignant human melanocytes show consistent changes in gene expression. *Recent Results Cancer Res.* 1995, *139*, 123–135.
- [11] Bernard, K., Litman, E., Fitzpatrick, J. L., Shellman, Y. G. *et al.*, Functional proteomic analysis of melanoma progression. *Cancer Res.* 2003, *63*, 6716–6725.
- [12] Han, M. J., Herlyn, M., Fisher, A. B., Speicher, D. W., Microscale solution IEF combined with 2-D DIGE substantially enhances analysis depth of complex proteomes such as mammalian cell and tissue extracts. *Electrophoresis* 2008, *29*, 695–705.
- [13] Juhasz, I., Albelda, S. M., Elder, D. E., Murphy, G. F. *et al.*, Growth and invasion of human melanomas in human skin grafted to immunodeficient mice. *Am. J. Pathol.* 1993, *143*, 528–537.
- [14] Zuo, X., Echan, L., Hembach, P., Tang, H. Y. *et al.*, Towards global analysis of mammalian proteomes using sample prefractionation prior to narrow pH range two-dimensional gels and using one-dimensional gels for insoluble and large proteins. *Electrophoresis* 2001, *22*, 1603–1615.
- [15] Zuo, X., Speicher, D. W., Comprehensive analysis of complex proteomes using microscale solution isoelectrofocusing prior to narrow pH range two-dimensional electrophoresis. *Proteomics* 2002, *2*, 58–68.
- [16] Tang, H. Y., Ali-Khan, N., Echan, L. A., Levenkova, N. *et al.*, A novel four-dimensional strategy combining protein and peptide separation methods enables detection of low-abundance proteins in human plasma and serum proteomes. *Proteomics* 2005, *5*, 3329–3342.
- [17] Omenn, G. S., States, D. J., Adamski, M., Blackwell, T. W. *et al.*, Overview of the HUPO Plasma Proteome Project: results from the pilot phase with 35 collaborating laboratories and multiple analytical groups, generating a core dataset of 3020 proteins and a publicly-available database. *Proteomics* 2005, *5*, 3226–3245.
- [18] Speicher, D. W., Lee, K., Tang, H. Y., Echan, L. *et al.*, in: Ashcroft, A. E., Brenton, G., Monaghan, J. J. (Eds.), *Advances in Mass Spectrometry*, Elsevier Science, New York 2004, pp. 37–57.
- [19] Madoz-Gurpide, J., Canamero, M., Sanchez, L., Solano, J. *et al.*, A proteomics analysis of cell signaling alterations in colorectal cancer. *Mol. Cell. Proteomics* 2007, *6*, 2150–2164.
- [20] Nicholson, B. E., Frierson, H. F., Conaway, M. R., Seraj, J. M. *et al.*, Profiling the evolution of human metastatic bladder cancer. *Cancer Res.* 2004, *64*, 7813–7821.
- [21] Riker, A. I., Enkemann, S. A., Fodstad, O., Liu, S. *et al.*, The gene expression profiles of primary and metastatic melanoma yields a transition point of tumor progression and metastasis. *BMC Med. Genomics* 2008, *1*, 13.
- [22] Boyd, A. S., Shakhtour, B., Shyr, Y., Minichromosome maintenance protein expression in benign nevi, dysplastic nevi, melanoma, and cutaneous melanoma metastases. *J. Am. Acad. Dermatol.* 2008, *58*, 750–754.
- [23] Sinha, P., Kohl, S., Fischer, J., Hutter, G. *et al.*, Identification of novel proteins associated with the development of chemoresistance in malignant melanoma using two-dimensional electrophoresis. *Electrophoresis* 2000, *21*, 3048–3057.
- [24] Sinha, P., Poland, J., Kohl, S., Schnolzer, M. *et al.*, Study of the development of chemoresistance in melanoma cell lines using proteome analysis. *Electrophoresis* 2003, *24*, 2386–2404.
- [25] Bjorkdahl, O., Dohlsten, M., Sjogren, H. O., Vaccination with B16 melanoma cells expressing a secreted form of interleukin-1beta induces tumor growth inhibition and an enhanced immunity against the wild-type B16 tumor. *Cancer Gene Ther.* 2000, *7*, 1365–1374.
- [26] Apte, R. N., Dotan, S., Elkabets, M., White, M. R. *et al.*, The involvement of IL-1 in tumorigenesis, tumor invasiveness, metastasis and tumor-host interactions. *Cancer Metastasis Rev.* 2006, *25*, 387–408.
- [27] Weston, C. R., Davis, R. J., The JNK signal transduction pathway. *Curr. Opin. Cell Biol.* 2007, *19*, 142–149.
- [28] Kennedy, N. J., Davis, R. J., Role of JNK in tumor development. *Cell Cycle* 2003, *2*, 199–201.
- [29] Sakurai, T., Maeda, S., Chang, L., Karin, M., Loss of hepatic NF-kappa B activity enhances chemical hepatocarcinogenesis through sustained c-Jun N-terminal kinase 1 activation. *Proc. Natl. Acad. Sci. USA* 2006, *103*, 10544–10551.
- [30] Hipfner, D. R., Cohen, S. M., Connecting proliferation and apoptosis in development and disease. *Nat. Rev. Mol. Cell Biol.* 2004, *5*, 805–815.
- [31] Kraehn, G. M., Utikal, J., Udart, M., Greulich, K. M. *et al.*, Extra c-myc oncogene copies in high risk cutaneous malignant melanoma and melanoma metastases. *Br. J. Cancer* 2001, *84*, 72–79.
- [32] Simon, H. G., Risse, B., Jost, M., Oppenheimer, S. *et al.*, Identification of differentially expressed messenger RNAs in human melanocytes and melanoma cells. *Cancer Res.* 1996, *56*, 3112–3117.
- [33] Boon, K., Caron, H. N., van Asperen, R., Valentijn, L. *et al.*, N-myc enhances the expression of a large set of genes functioning in ribosome biogenesis and protein synthesis. *EMBO J.* 2001, *20*, 1383–1393.
- [34] LaBonne, C., Bronner-Fraser, M., Molecular mechanisms of neural crest formation. *Annu. Rev. Cell. Dev. Biol.* 1999, *15*, 81–112.
- [35] Bartenjev, I., Rudolf, Z., Stabuc, B., Vrhovec, I. *et al.*, Cathepsin D expression in early cutaneous malignant melanoma. *Int. J. Dermatol.* 2000, *39*, 599–602.
- [36] Frohlich, E., Schlagenhauff, B., Mohrle, M., Weber, E. *et al.*, Activity, expression, and transcription rate of the cathepsins B, D, H, and L in cutaneous malignant melanoma. *Cancer* 2001, *91*, 972–982.
- [37] Khan, A., Krishna, M., Baker, S. P., Malhotra, R., Banner, B. F., Cathepsin B expression and its correlation with tumor-associated laminin and tumor progression in gastric cancer. *Arch. Pathol. Lab. Med.* 1998, *122*, 172–177.
- [38] Foekens, J. A., Look, M. P., Bolt-de Vries, J., Meijer-van Gelder, M. E. *et al.*, Cathepsin-D in primary breast cancer:

- prognostic evaluation involving 2810 patients. *Br. J. Cancer* 1999, 79, 300–307.
- [39] Andreasen, P. A., Egelund, R., Petersen, H. H., The plasminogen activation system in tumor growth, invasion, and metastasis. *Cell. Mol. Life Sci.* 2000, 57, 25–40.
- [40] Mueller, B. M., Yu, Y. B., Laug, W. E., Overexpression of plasminogen activator inhibitor 2 in human melanoma cells inhibits spontaneous metastasis in scid/scid mice. *Proc. Natl. Acad. Sci. USA* 1995, 92, 205–209.
- [41] Shimizu, T., Sato, K., Suzuki, T., Tachibana, K., Takeda, K., Induction of plasminogen activator inhibitor-2 is associated with suppression of invasive activity in TPA-mediated differentiation of human prostate cancer cells. *Biochem. Biophys. Res. Commun.* 2003, 309, 267–271.
- [42] Ramont, L., Pasco, S., Hornebeck, W., Maquart, F. X., Monboisse, J. C., Transforming growth factor-beta1 inhibits tumor growth in a mouse melanoma model by down-regulating the plasminogen activation system. *Exp. Cell Res.* 2003, 291, 1–10.
- [43] Evan, G. I., Vousden, K. H., Proliferation, cell cycle and apoptosis in cancer. *Nature* 2001, 411, 342–348.
- [44] Asher, G., Lotem, J., Cohen, B., Sachs, L., Shaul, Y., Regulation of p53 stability and p53-dependent apoptosis by NADH quinone oxidoreductase 1. *Proc. Natl. Acad. Sci. USA* 2001, 98, 1188–1193.